International Journal of Scientific Engineering and Technology
Volume No.5 Issue No.4, pp: 173-179

ISSN:2277-1581
01 April 2016

Experimental Characterisation of Cation-exchange Resin for Biomass Green Solvent Production

Edidiong Okon, Habiba Shehu, Ifeyinwa Orakwe, Ngozi Nwogu, Mohammad Kajama and Edward Gobina*.

Center for Process Integration and Membrane Technology (CPIMT), School of Engineering. The Robert Gordon University Aberdeen, AB10 7GJ, United Kingdom.

Corresponding Author: e.gobina@rgu.ac.uk

Abstract*—In this work, resin catalysts used for lactic acid esterification was analysed using liquid N_2 adsorption-desorption isotherm measured at 77 K using an automated adsorption instrument (Quantachrome 2013). The surface area and pore size distribution were obtained using the BET** (Brunauer-Emmett-Teller) ***and BJH (Barrette – Joyner Halenda) methods of the N_2 desorption isotherm respectively. The N_2 vapour adsorption data was determined at the vapour pressure range (P/P_o) of 0.05 – 0.1. An auto sampler Gas chromatograph equipped with mass spectrometer (GC-MS) was used for the analysis of the esterification reaction product. Fourier Transform Infrared - Attenuated Total Reflection (FTIR-ATR) was used for the structural identification of the component with the strongest adsorption strength on the surface of the resin catalysts. The results of the N_2 adsorption isotherm for the resin catalysts showed a type IV adsorption isotherm with hysteresis confirming a mesoporous layer in pore size the range of 2 – 5 nm. The multipoint method exhibited a straight line curve with a positive slope (552.42) and intercept (1.607). The BET surface area of the amberlyst 36 was found to be higher (20.171 m^2/g) than that of dowex 50W8x (0.497 m^2/g). These results were further confirmed by the gas chromatograph analysis where products of the amberlyst 36 was found to elute faster at the retention time of 1.521 mins in contrast to those of dowex50W8x resin catalysts. The result of the FTIR analysis of the resin catalysts showed that the band at 1731 cm^{-1} correspond to C-O stretching with strong adsorption bond while the band at 2992 cm^{-1} representing O-H corresponds to stretching vibration bond suggesting ethanol and lactic acid as the adsorption components on the surface of the resin catalysts. The gas chromatograph NIST library spectra of the esterification reaction products exhibited the structure of ethyl lactate (45) on the mass spectra with other compounds with their respective ions including formic acid (71) formic acid and 2,3-butandiol (73).

Keywords—Heterogeneous catalysts, characterisation, esterification, adsorption, ethyl lactate and cation-exchange resin.

I. Introduction

Solvent market plays a major role in all part of industrial manufacturing sector. The environmental and toxicological effects of solvents have become important in chemical processes. Because environmental problems have threatened the natural order and living health including climate change and global warming, a lot of research is being carried out to find the availability of more environmentally safe chemicals and processes [1]. Esterification reaction of alcohol with carboxylic acid in the presence of catalysts has attracted a lot of attention in the chemical industries. The ester products of this reaction are normally used in different chemical industries including flavour and fragrances, solvent of paints, pesticides, adhesives, emulsifiers and plasticizers [2],[3]. Besides the numerous applications, esters from nonedible crops and cultivated sources are potential candidates in carbon emission reduction. However, in order to ascertain the future energy supplies and offset the environmental impact, low-carbon technologies will play a major role in this regards. In addition to the energy efficiency, different types of renewable energy, nuclear power, carbon capture/storage as well as solar and geothermal technologies must be widely developed in order to reach the emission targets [3]. Ethyl lactate is an organic ester that can be obtained by reversible esterification of biomass-based fermented ethanol and lactic acid. It is a clear to yellow liquid, and it is found naturally in small quantities in food, wine, chicken and some fruits [4].

Due to numerous advantages in the replacement of this solvent over toluene and xylene, ethyl lactate has been described by Environmental Protection Agency (EPA) as green solvent [1]. Esters of carboxylic acids are important in a variety of products of ranging from perfumes to bio-fuels. The latter is of particular significance due to the finite nature of crude oil resources and environmental impact [5]. Since esterification reactions are extremely slow in the absence of catalysts, both heterogeneous and homogeneous have been used to catalysed the reaction [6],[3],[7]. Homogenous catalysts such as mineral acids and heterogeneous catalysts such as cation-exchange resin are commonly used in the liquid-phase esterification reactions in order to increase the yield of the reaction product. Although homogeneous catalysts have high catalytic activity, heterogeneous solid catalysts can be employed to solve the problems of homogeneous catalysts including equipment corrosion. Heterogeneous catalysts possess a lot of inherent advantages over dissolved electrolytes [6],[8]:

i. The catalysts can be easily removed from the reaction system by filtration.
ii. Purity of product is higher since side reactions can be eliminated or less significant.
iii. They can avoid corrosion problems
iv. They can be used repeatedly over a long duration with any deactivation.

In spite of numerous reports on esterification with heterogeneous catalysts, only very few kinetic study considers the effect of adsorption, reaction and diffusion in the heterogeneous system in contrast to the homogeneous system. As such, the reaction mechanisms and the rate expression are more complicated in heterogeneous catalysts compared to that of the homogeneous catalyst [9]. In several cases, esterification yield is normally limited by thermodynamic equilibrium. However, in some cases, the selectivity can also be improved to a specific product, ignoring the product distribution initiated by equilibrium.

ISSN:2277-1581
01 April 2016

Nevertheless, several conventional methods can be employed for increasing the yield of the reaction product including raising the pressure and temperature for such endothermic reaction to drive the reaction to a higher yield. Other methods seek to drive a reaction away for the equilibrium [10]. Aside from thermodynamic equilibrium limitation, reaction yield can also be limited by other factors such as mass transfer and heat generated during the esterification. Such limitations can be overcome by altering the reaction design to enhance the reaction yield [10]. According to Sharma et al. [11] the kinetics of the esterification reaction products can be analysed using two methods; either by titration or using GC with a choice of detector and carrier gas. Using the GC-MS, the product can be analysed by matching the retention time of the reaction product to the retention time of the commercial ethyl lactate. The adsorption isotherm is known to convey a great deal of information about the surface area and pore size distribution of the samples used for the investigation [12]. According to IUPAC (International Union of Pure and Applied Chemistry), the physisorption isotherm can be classified into six different types as explained below:

- Type 1 isotherm is characterised by the adsorption in the non-porous microporous region at a low relative pressure.
- Type ll is characteristic of non-porous or macroporous adsorbents with the formation of a multilayer of adsorbate (gas molecule) on the surface of the adsorbent.
- Type III is characteristic of a non-porous or macroporous layer with weak interaction between the gas molecule and the membrane material.
- Type IV isotherm reflects a macroporous material which involves the coverage of the monolayer –multilayer on the external and mesoporous surface which is followed by capillary condensation in the mesoporous region with the formation of several hysteresis loop based on the shape of the pores.
- Type V isotherm is characteristic of a mesoporous material and involves the weak interaction between the permeating gas molecule and the membrane material.
- Type V1 isotherm takes place in a highly uniform surface [13]. During the specific surface area analysis of the internal and external surface of porous material using physical gas adsorption, the amount of gas adsorbed depends on the relative vapour pressure [13].

THEORY

In esterification, where an excess of the alcohol is used, if the selectively of the desired product is 100 % the conversion of the limiting reactant of the acid ‘’X’’ can be given as the ratio of the acid to ester.

$$\frac{\text{Acid}}{\text{Ester}} = R_1 = \frac{1-X}{X} \quad \text{.....(1)}$$

Where R_1 represent the ester group. Making X the subject of the formula:

$$X = \frac{1}{R_1+1} \quad \text{.....(2)}$$

In the pervaporation aided esterification, the ratio of ester to water is equivalent to the equation:

$$\frac{Ester}{Water} = R_2 = \frac{X}{Y} \quad \text{.....(3)}$$

Where R_2 = alkyl group

Making Y the subject of the formula

$$Y = \frac{X}{R_2} \quad \text{.....(4)}$$

Thus, using the calculated X and Y values from the experimentally determined concentrations, the amount of water removed from the esterification reaction system (N_w) can be calculated using the formula:

$N_w = N_i\,(X-Y)$ (mol) .....(5)

Where Ni = initial amount of lactic acid, N_w = amount of water removed, X and Y are the concentration of lactic acid values (mol).

The volume of the liquid phase reaction change from the feed volume V_o to V_1. If the volume of the removed water is V_2 , then Vo which the feed volume can be calculated using the formula;

$V_o = V_1 + V_2$ .....(6)

Making V_2 the subject of the formula and multiplying by the with initial amount of lactic acid (N_o) and the X and Y concentration values, then the equation can be written as:

$V_2 = V_1 * N_o\,(X-Y)$ .....(7)

Where V_1 = the molar volumes of the liquid.

For first order characteristic of the reactant and products, the rate (r_{ester}) of the reversible esterification can be written as:

$$r_{ester} = K_1\left[\frac{N_o(1-X)}{V_1}\right]\left[\frac{N_o(R_1-X)}{V_1}\right] - \frac{K_1}{K_{eq}}\left[\frac{NoX}{V_1}\right]\left[\frac{NoY}{V_1}\right] \quad \text{.....(8)}$$

Where r_{ester} = rate of ester production and consumption, Keq = equilibrium constants X and Y are the concentration values of lactic acid (mols). V_1 = molar volume of the liquid.

If we multiply although by $\frac{N_i K_1}{V_1}$ the change in molar balance for a batch reactor (x) at time ‘’t’’ will result in:

$$\frac{dx}{dt} = \frac{N_o K_1}{V_1} * \left[(1-x).(R_1 - X) - \frac{X.Y}{K_{eq}}\right] \quad \text{.....(9)}$$

The equilibrium constant, K_{eq} is obtained from the composition of the reaction mixture in the batch experiment without removal of water (so $R_2 = 1$, Y = X and $V_1 = V_O$) at equilibrium.

Thus the equilibrium constant K_{eq} can be written as:

$$K_{eq} = \left[\frac{[E][W]}{[A][B]}\right]eq \quad \text{.....(10)}$$

II. Material and Methodology

The forward rate constant K_1 is determined from the early stage of the reaction (t = 0). In the coupled reaction system (separation

ISSN:2277-1581
01 April 2016

and reaction in one unit), the water removal rate at time ''t'' can be expressed as:

$$R_{H20} = \frac{dN_W}{dt} = N_i \frac{d(X-Y)}{dt} \left(\frac{mol}{min}\right) \quad \text{.....(12)}$$

However, if all the water is removed through the membrane, the flux can be calculated using the formula:

$$J = \frac{R_{H20}}{A} \quad \text{.....(13)}$$

Where J = water flux through the membrane ($molms^{-1}$), A = effective membrane surface area (m), R_{H20} = rate of water removal ($Kmols^{-1}$) [14].

Material

Aqueous lactic acid (99.9 wt%) and ethanol (99.9 wt%) solutions were purchased from Sigma-Aldrich, UK and were used as received without further purification. The catalysts used in the experiments were commercial solid cation-exchange resins purchased from Sigma-Aldrich, UK. The deionised water used for the washing of the catalysts was supply by the Centre for Process Integration and Membrane Technology (CIPMT), Robert Gordon University (RGU), Aberdeen, UK. The 500mL batch reactor, reflux condenser and the vacuum pump used for the esterification process were all purchased from Sigma Aldrich, UK.

A. Catalysts Cleaning

Prior to the esterification process, the fresh commercial cation-exchange resin was weighed into a 50 mL beaker and was rinsed with 2 mL of deionised water with 10 mL of ethanol. The catalysts were reweighed and oven dried at 65 ^{o}C for 24 hrs to remove any poisonous substances and moisture completely. The catalysts cleaning process was carried out based on a similar method by Jogunola et al [15].

B. Batch Process Esterification

Figure 1 shows the batch process esterification reaction set-up. After the catalyst cleaning process, 30 mL of lactic acid with 5g of the different cation-exchange resins were charged into the reactor and heated to 60, 80 and 100 ^{o}C. After the desired temperature was reached, 50 mL of ethanol which has been heated separately using the heating mantle was added to the mixture. The stirring and heating of the reaction mixture was achieved using a magnetic hot plate with a stirrer. The stirrer speed was controlled at the speed of about 400-800 rpm. The water from the reaction product was removed by connecting two vacuum pumps to the openings of the reactor i.e the inlet and the outlet water flow. The inlet water flows through the pump was used to flush the evaporated system while the outlet water displaced the waste water from the reaction system as shown in figure 1. The mixture was left in the reactor with the magnetic stirrer to mix the solution together before the analysis. This experiment was carried out in the fume cupboard. After the esterification process, about 1mL of the sample was injected to the GC-MS for the qualitative analysis.

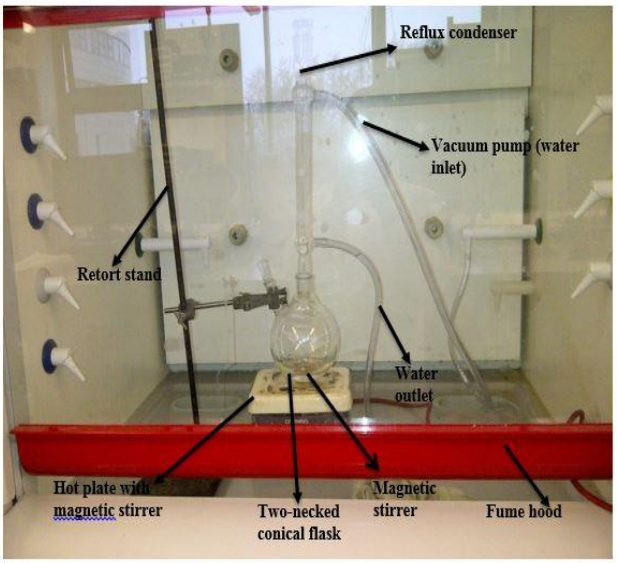

Figure 1: Batch process Esterification process set-up.

C. *Instrumentation*

Prior to the liquid nitrogen degassing process, about 0.1g of the cation-exchange sample was measured into the sample cell. After the degassing process, of the sample was loaded unto the liquid nitrogen instrument. The adsorption isotherms were obtained by dosing the nitrogen (99.99% purity) onto the catalyst contained within a liquid nitrogen bath at 77 K. A similar method to that of Teo and Saha [12] was adopted with some modification in the catalyst degassing temperature and time. The helium and nitrogen gas pressures were set at 7 and 5 bar respectively. The rate of the sample analysis was 10 ^{o}C/minutes whereas the analysis time was set for 6 hrs at 300 ^{o}C. The liquid nitrogen adsorption temperature was programmed at 77 K. Thermo Scientific Fourier transform infrared coupled with attenuated total reflection (Nicolet iS10 FTIR-ATR) was used for the structural analysis of the resins. This method was used in order to determine the phenomenon of the component with the strongest absorption strength on the surface of the resin catalysts. The FTIR results interpretation was done using the characteristic library spectra provided by the school of pharmacy life science, Robert Gordon University, UK. Agilent 7890B autosampler Gas chromatograph (GC) system coupled with Agilent technologies 5977A mass spectrometer (MSD) was used for the analysis of the esterification product. The NIST GC software program was used for data collection while Helium gas (99.98 % purity) was used as the carrier gas. The surface morphological examination of the resin catalyst was carried out using scanning electron microscopy (The Zeiss EVO LS10) coupled with energy dispersive x-ray analyser (The Oxford INCA system).

Figure 2a and b shows the Liquid nitrogen adsorption and gas chromatograph instruments that were used for the characterisation process.

doi : 10.17950/ijset/v5s4/403

ISSN:2277-1581
01 April 2016

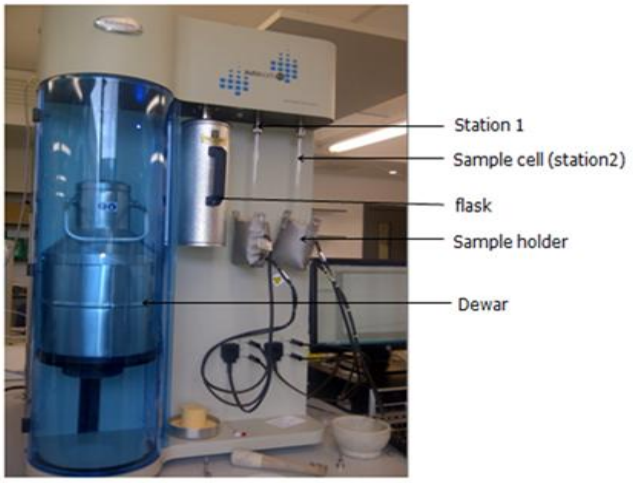

(a)

(b)

Figure 2a and b: Pictorial view of the Quantachrome 2013 liquid nitrogen adsorption-desorption (a) Agilent 7890B autosampler Gas chromatography (GC) system coupled with Agilent 5977A mass spectrometry detector (MSD) (b) at the Centre for Process Integration and Membrane Technology (CPIMT), RGU.

III. Results and Tables

A. Liquid nitrogen adsorption of catalysts

Figure 3 depicts the BET surface area and BJH curves for amberlyst 36 cation-exchange resin at the liquid nitrogen temperature of 77 K. Table 1 shows the average pore diameter, pore volume, surface area of the resin catalysts. From figure 3a, it was found that the BET result for amberlyst 36 resin catalysts showed a higher surface area (20.171 m^2/g) than dowex 50W8x (0.497 m^2/g) as shown in table 1, which confirmed catalytic activity of amberlyst 36 catalysts in the removal of water from the esterification product as this catalysts also elutes faster in the GC-MS analysis. However a positive slope and intercept were also obtained for the two catalysts as shown in table 1. The increasing order BET surface area of the resin catalysts was amberlyst 36 (20.171 m^2/g) > dowex 50W8x (0.497m^2/g). From the BET results obtained figure 3a and b, it was found that the BET curves for both amberlyst 36 and dowex 50W8x cation-exchange resins exhibited a type IV isotherm with hysteresis loop on the curve indicating a mesoporous material [4],[16]. However, the results were found to be in good agreement with that reported in the literature for these type of materials [16].

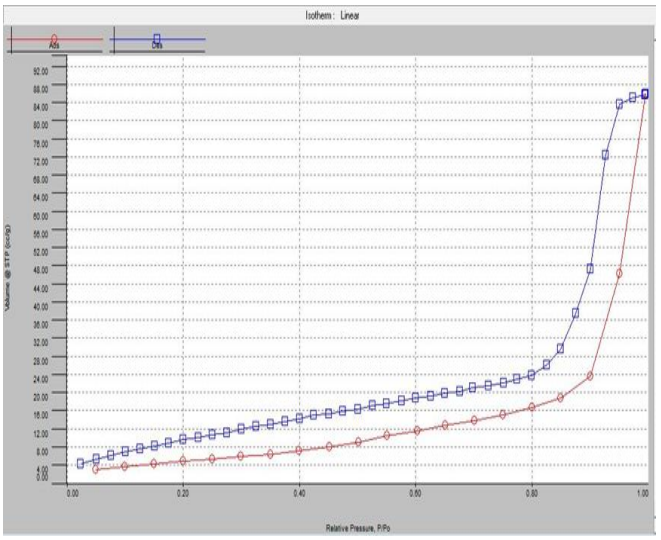

Figure 3a: BET isotherm for amberlyst 36 at 77 K

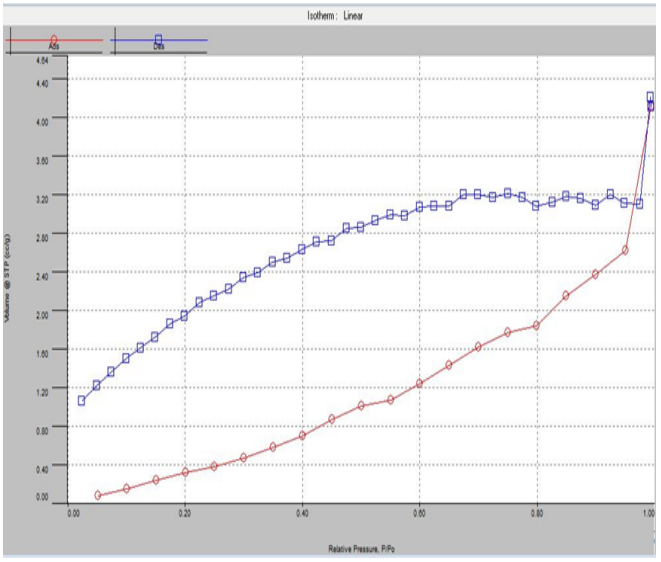

Figure 3b: BET isotherm for dowex 50W8x at 77 K

Table 1: BET surface area, BJH average pore diameter, pore volume, slope and intercept of the amberlyst 36 and dowex 50W8x resin catalysts.

Cation-exchange resin	BET Surface area(m^2/g)	BJH Pore diameter (nm)	Pore Volume(cc/g)	Slope	Intercept
Amberlyst 36	20.171	3.320	0.125	522.42	$1.607*10^{-1}$
Dowex 50W8x	0.497	3.708	0.004	11309.29	$4.26*10^{-3}$

ISSN:2277-1581
01 April 2016

The average pore diameter, the slope, intercept as well as the pore volume of the resin catalysts were obtained using BJH methods of the liquid nitrogen adsorption at 77 K. Figure 4 shows the BJH curves for amberlyst 36 and dowex 50W8x. From figure 4a and b, it was found that although dowex 50W8x exhibited a lower surface area than amberlyst 36. The pore diameter of dowex 50W8x was observed to be a bit higher (3.708) suggesting that the resin catalysts also show a good performance in the esterification but the surface area is lower due to the higher concentration of lactic acid that penetrate the catalyst pores in the course of the reaction. From figure 4a it was suggested that the higher pore diameter of amberlyst 36 catalyst possess a strong catalytic effect for the reactant solvent to diffuse into the pores during the esterification process. Although the dowex 50W8x showed a lower surface area, the pore diameter of this catalyst was still found to be in the range of 2 -50 nm which is consistent for mesoporous classification of the adsorption isotherm.

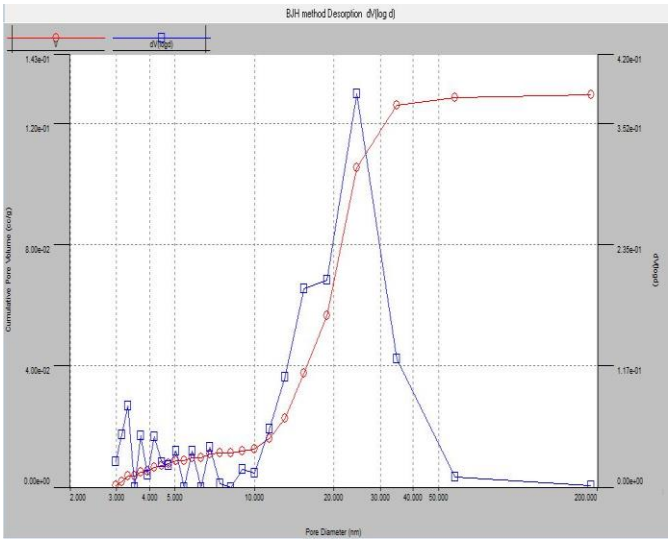

Figure 4b: BHJ for amberlyst 36 at 77 K.

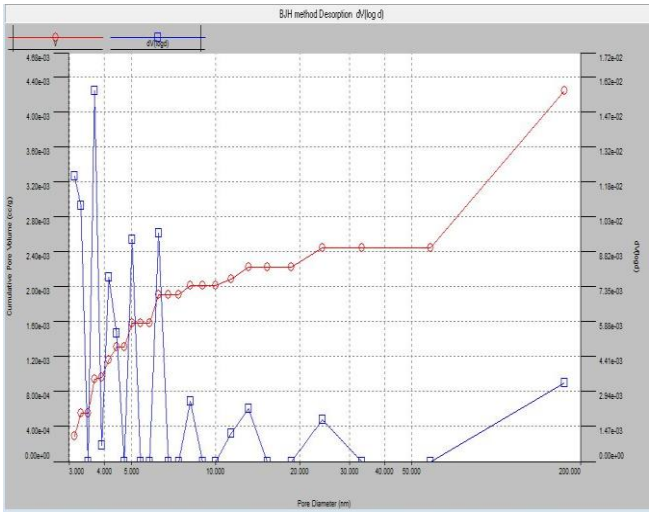

Figure 4b: BHJ for dowex 50W8x at 77 K.

B. SEM/EDXA analysis of catalysts

Figure 5 depicts the SEM surface morphology of amberlyst 36 and Dowex 50W8x resin catalysts at 100 ^{o}C. The surface examination of the catalysts was carried out between the scale range of 10 -100 µm. The images were analysed at the magnification of 100 X at the working distance of 8.5 mm while the chamber pressure was set between the range of 100 -101 Pa. From the results of the SEM of the resin catalysts, it was found that the surface morphology of dowex 50W8x (b) showed a clear surface with no crack. Although amberlyst 36 also exhibited a clear surface, there was some evidence of perturbations on the surface suggested to be as the result of the effect of the effect of temperature and high concentration of lactic acid on the surface of the resin catalyst after the esterification process.

It was also found that dowex 50W8x exhibited a larger pore on the surface in contrast to amberlyst 36. The EDXA was used to determine the elemental composition of cation-exchange resin catalysts. The result obtained from the EDXA of the resin catalysts confirmed that there was an even distribution of the different elements including sulphur (S), Aluminium (Al), titanium (Ti), carbon (C) and oxygen (O) in the material.

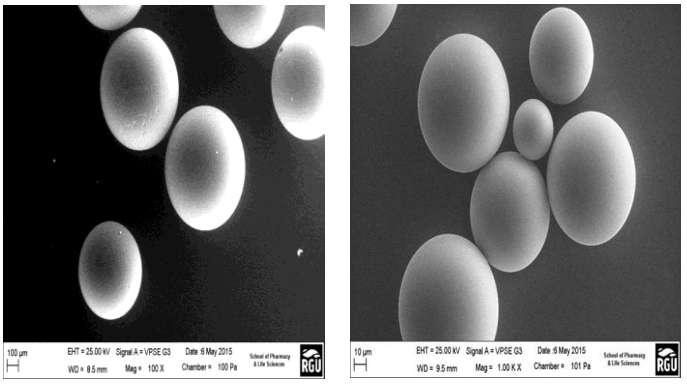

(a) Amberlyst 36 at 100^{o}C (b) Dowex 50W8x at 100.

Figure 5a and b: SEM surface image of amberlyst 36 (a) and dowex50W8x after the esterification process.

C. GC-MS Analysis of resin catalyst

Figure 6 present the ion chromatogram of the cation-exchange resin catalysts at 100 ^{o}C. From figure 6a, it can be seen that the esterification product elutes first and has that the retention time of 1.521 min with the peak area of 1281027774 m^2. However, the last elution time was found to occur at 9.142 min with the peak area of 99059728 m^2. It was found that as the solvent elution time increases, the peak area increases.

ISSN:2277-1581
01 April 2016

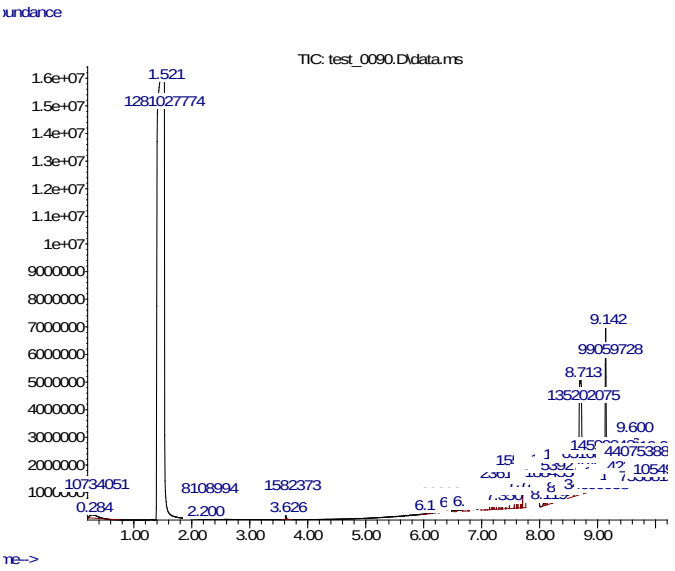

Figure 6b: Ion chromatogram for amberlyst 36 at 100 ^{o}C.

Figure 6b shows the NIST mass spectra for the esterification reaction product. From figure 6b, it was found that the reaction product exhibited the structure of ethyl lactate at ion number 45 with the highest peak on the spectra as expected which was in agreement with the library spectra for the commercial ethyl lactate solvent. The NIST data was also used to detect the different ions with their respective peaks on the spectra. However, other products were also found on the spectra including methyl methanethiosulphonate (43), 2,4-pentanedio (44)l, methylazoxymthanol acetate (46), hydroxylamine, o-methyl (53), acetaldehyde, methoxy (56), methylal (58), acetoin (61), formic acid (71), 2,3-butandiol (73), oxirane (75), propane 2-fluoro (76), 2-butanediol (89) and ethanol,2methoxy (91). It was suggested that the presence of these compounds could have occurred as a results of some impurities from lactic acid on interaction with the strong cation-exchange resins.

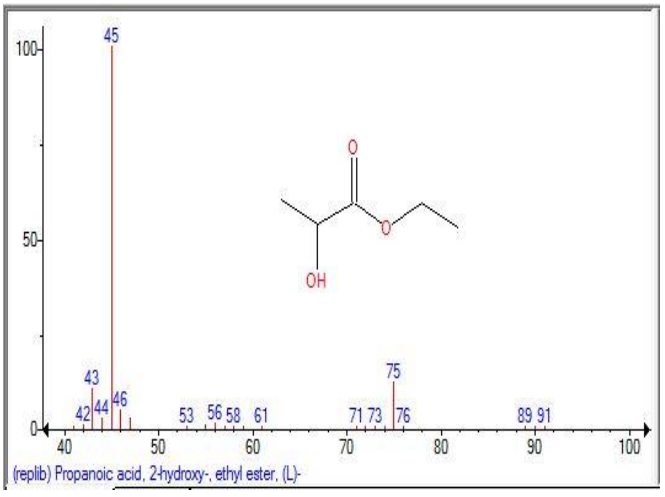

Figure 6b: Mass spectra for amberlyst 36 cation-exchnage resin

D. FTIR/ATR analysis of catalysts

Figure 7 presents the FTIR spectra for the cation-exchange resin. From figure 7, it was observed that the FTIR analysis of the resin catalysts showed the band at 1731 cm^{-1} corresponding to C-O stretching strong adsorption bond, and the band at 2992 cm^{-1} representing O-H stretching vibration bond. However, the band at 1204 cm^{-1} was observed to represent = C – O – C- structure. This (=C-O-C-) structure was suggested to originate from the carboxylic acid functional group while the O-H suggested to occur from the alcohol functional group. It was suggested that the strong adsorption bond of C-O and O-H could indicate the fact that ethanol and lactic acid as the adsorption component on the surface of the resin catalysts [7],[17].

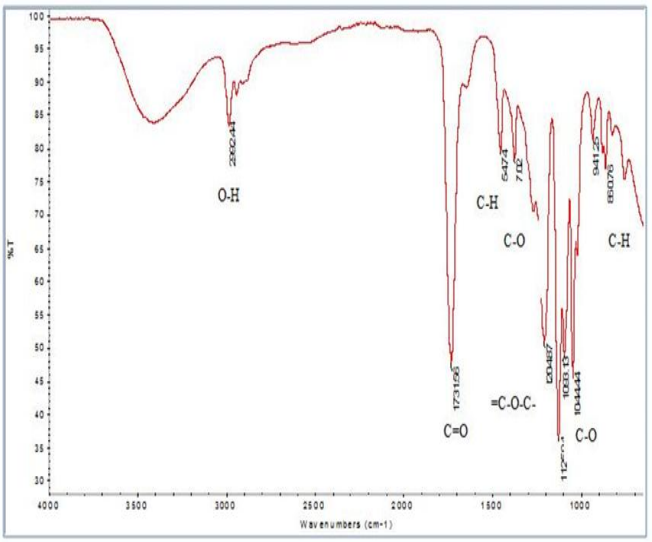

Figure 7: FTIR-ATR spectra for amberlyst 36 at 60 ^{o}C .

IV. Conclusion

The characterisation of the resin catalysts have been carried out using different methods including SEM/EDXA, FTIR, Liquid nitrogen adsorption and the esterification reaction product catalysed by the catalysts was analysed using GC-MS. Amberlyst 36 catalyst reveal itself as the most stable and most effective catalysts in esterification reaction in contrast to dowex 50W8x catalysts in the equilibrium process of ethyl lactate. FTIR analysis of the resin catalysts detected C=O and O = H functional groups which confirms the presence of ethanol and lactic acid as the strongest components of the surface of the resin catalysts. The amberlyst 36 resin catalyst showed a higher surface area and pore diameter in contract to dowex50W8x. The pore size of the resin catalysts was found to be in the mesoporous region as confirmed by the adsorption isotherm classification of such material. The resin catalyst exhibited the first elution at 1.521 min with peak area of 1281027774 m^{2}. The mass spectra of the esterification product was identified to be that of ethyl lactate in accordance with the of the commercial ethyl lactate. The NIST mass spectra of the GC-MS exhibited other component on the spectra including acetoin and oxirane. The SEM surface image dowex 50W8x exhibited a larger pore on the surface in contrast to amberlyst 36. Amberlyst 36 was found to most effective in the removal of water from the esterification reaction process.

Acknowledgements

The Authors acknowledge the Center for Process Integration and Membrane Technology (CPIMT) at RGU for providing the research infrastructure, School of Pharmacy and Life science for the SEM image. CCMEC is also acknowledge for their financial support towards the research.

Nomenclature

Symbols

A = Surface area of the membrane (m^2)
J = Flux (mol s^{-1} m^{-2})
Q_i = Permeance (mol m^{-2} s^{-1} Pa^{-1})
M = Gas molecular weight (g/mol)
Q = Gas flow rate (mol s^{-1})
T = Temperature (Kelvin)
ΔP = Transmembrane Pressure drop (bar).
R_1 = Alkyl group
R_2 = Alkyl group
N_i = Initial amount of lactic acid
N_w = Amount of water
X = Concentration of lactic acid values (mol)
Y = Concentration of lactic acid values (mol)
N_o = Initial amount of lactic
V_1 = The molar volume of liquid
V_2 = The molar volume of liquid
r_{ester} = Rate of ester production and consumption
K_{eq} = Equilibrium constant
R_{H2O} = Rate of water removal ($mols^{-1}$)
A = Surface area of the membrane (m^2).

References

i. Ugur Nigiz F, Durmaz Hilmioglu N. Green solvent synthesis from biomass based source by biocatalytic membrane reactor. International Journal of Energy Research. 2015; .

ii. Toor AP, Sharma M, Thakur S, Wanchoo RK. Ion-exchange Resin Catalyzed Esterification of Lactic Acid with Isopropanol: a Kinetic Study. Bulletin of Chemical Reaction Engineering & Catalysis. 2011; 6(1).

iii. de Paiva, Eduardo Jose Mendes, Sterchele S, Corazza ML, Murzin DY, Wypych F, Salmi T. Esterification of fatty acids with ethanol over layered zinc laurate and zinc stearate–Kinetic modeling. Fuel. 2015; 153:445-454.

iv. Pereira CS, Silva VM, Rodrigues AE. Ethyl lactate as a solvent: properties, applications and production processes–a review. Green Chemistry. 2011; 13(10):2658-2671.

v. Miao S, Shanks BH. Esterification of biomass pyrolysis model acids over sulfonic acid-functionalized mesoporous silicas. Applied Catalysis A: General. 2009; 359(1):113-120.

vi. Çitak A. Application of Ion Exchange Resins in the Synthesis of Isobutyl Acetate. Ion Exchange Technology II. : Springer; 2012. p. 137-148.

vii. Sert E, Buluklu AD, Karakuş S, Atalay FS. Kinetic study of catalytic esterification of acrylic acid with butanol catalyzed by different ion exchange resins. Chemical Engineering and Processing: Process Intensification. 2013; 73(0):23-28.

viii. Kaur K, Wanchoo RK, Toor AP. Sulfated Iron Oxide: A Proficient Catalyst for Esterification of Butanoic Acid with Glycerol. Industrial & Engineering Chemistry Research. 2015; 54(13):3285-3292.

ix. Sharma M, Wanchoo RK, Toor AP. Adsorption and kinetic parameters for synthesis of methyl nonanoate over heterogeneous catalysts. Industrial & Engineering Chemistry Research. 2012; 51(44):14367-14375.

x. Armor JN. Overcoming equilibrium limitations in chemical processes. Applied Catalysis A: General. 2001; 222(1–2):91-99.

xi. Sharma M, Wanchoo R, Toor AP. Amberlyst 15 Catalyzed Esterification of Nonanoic Acid with 1-Propanol: Kinetics, Modeling, and Comparison of Its Reaction Kinetics with Lower Alcohols. Industrial & Engineering Chemistry Research. 2014; 53(6):2167-2174.

xii. Teo H, Saha B. Heterogeneous catalysed esterification of acetic acid with isoamyl alcohol: kinetic studies. Journal of Catalysis. 2004; 228(1):174-182.

xiii. Weidenthaler C. Pitfalls in the characterization of nanoporous and nanosized materials. Nanoscale. 2011; 3(3):792-810.

xiv. Khajavi S, Jansen JC, Kapteijn F. Application of a sodalite membrane reactor in esterification—Coupling reaction and separation. Catalysis Today. 2010; 156(3):132-139.

xv. Jogunola O, Salmi T, Wärnå J, Mikkola J-. Kinetic and diffusion study of acid-catalyzed liquid-phase alkyl formates hydrolysis. Chemical Engineering Science. 2012; 69(1):201-210.

xvi. Miao S, Shanks BH. Mechanism of acetic acid esterification over sulfonic acid-functionalized mesoporous silica. Journal of Catalysis. 2011; 279(1):136-143.

xvii. Zhang Y, Ma L, Yang J. Kinetics of esterification of lactic acid with ethanol catalyzed by cation-exchange resins. Reactive and Functional Polymers. 2004; 61(1):101-114.